DESY Summer Programme

Fernando Romero López, University of Valencia, Spain

September 7, 2015

Abstract

This is a brief summary of my experience as a Summer Student at DESY. I worked under the supervision of Jürgen Reuter and Christian Weiss on the validation of `WHIZARD` , an event simulator. My tasks included the calculation of cross sections for some exemplary processes, in order to test and possibly improve the performance of `WHIZARD` .

Contents

1 Introduction and Motivation

This brief report is a summary of my experience as a summer student at DESY. Apart from the various and interesting lectures we had, I did a research internship in the Theory Group under the supervision of Jürgen Reuter and Christian Weiss. The topic of the my work was the use and validation of `WHIZARD` [5, 6], a program system designed for the efficient calculation of multi-particle scattering cross sections and simulated event samples.
`WHIZARD` can be linked to other programs such as Openloops [3] for loop matrix elements and FastJet [7], which provides clustering algorithms. The former is a fully automated implementation of the Open Loops algorithm for the fast numerical evaluation of tree and one-loop matrix elements for any Standard Model process, and the latter is a software package for jet finding in $p\ p$ and $e^+\ e^-$ collisions.
The goal of my project is the utilization of `WHIZARD` to reproduce results from the literature and other software such as MadGraph [8], in order to find possible bugs or improvements. The focus will be put in processes at so-called QCD Next-to-Leading-Order (NLO), which involves diagrams with exactly one additional strong coupling. In the following section some exemplary processes will be studied.

2 Validating `WHIZARD` and Openloops

2.1 $e^+\ e^- \to u\ \bar{u}\ g$

At Leading Order (LO), this process is made up from the Feynman diagrams below:

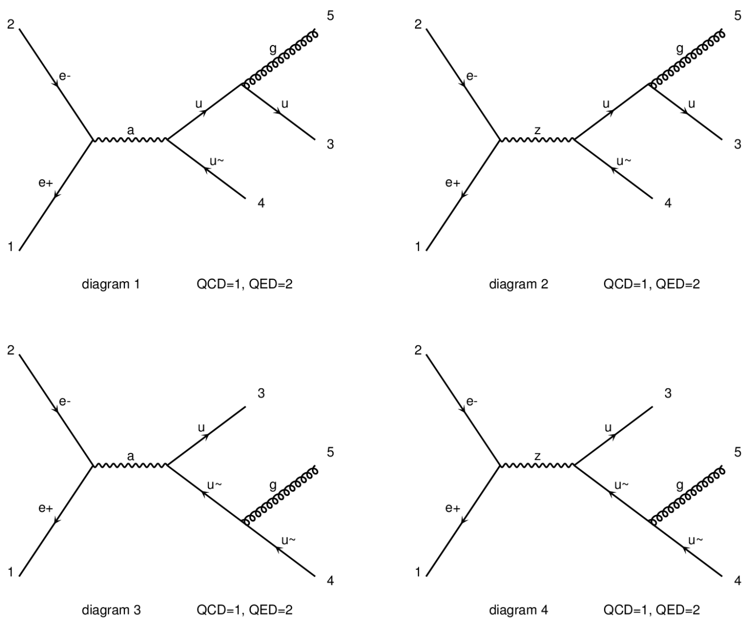

Figure 1: LO Feynman diagrams generated with MadGraph for $e^+\ e^- \to u\ \bar{u}\ g$.

However, the matrix elements for this one are divergent already at LO. In order to study this in more detail, let's focus on the first diagram in Figure 1:

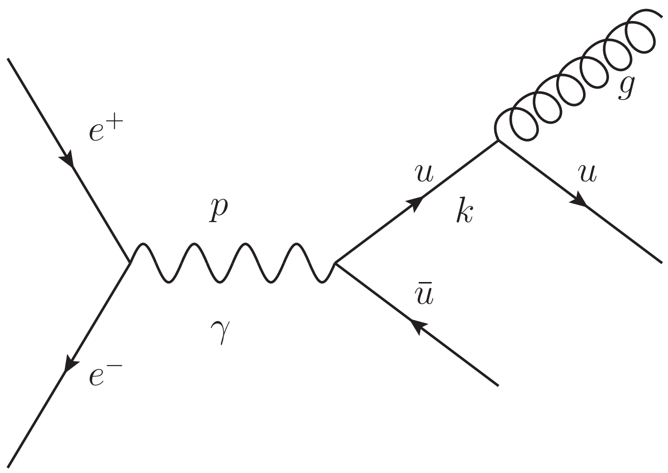

Figure 2: One of the LO Feynman diagrams for $e^+ \; e^- \to u \; \bar{u} \; g$.

Considering the up quark to be massless, the matrix element for the diagram in Figure 2 has the form:

$$\mathcal{M} = \alpha_s \alpha_e^2 \epsilon_\rho^* \left(\bar{e}\gamma_\mu e\right) \left(\frac{1}{p^2}\bar{u}\gamma^\mu \frac{\not{k}}{k^2}\gamma^\rho u\right). \tag{1}$$

In Equation 1, α_s and α_e are the strong and EW coupling constants and ϵ_ρ^*, the polarization vector of the gluon. Besides p and k are the 4-momentum of the photon and quark propagator respectively and u and e, the spinors of the fermions involved, as can also be seen in Figure 2 . The term corresponding to the quark propagator is the source of divergence. Taking into account that the 4-momentum of the propagator is $k = p_u + p_g$, that term becomes:

$$\frac{\not{k}}{k^2} = \frac{\not{k}}{2p_u p_g} = \frac{\not{k}}{2p_u^0 p_g^0 (1 - \cos\theta)}. \tag{2}$$

This term clearly diverges when $p_u^0 = 0$, $p_g^0 = 0$ or $\theta = 0$. The divergence due to the first two members is called soft divergence, due to the vanishing energy of the emitted particle, and the one coming from the latest is called collinear divergence, and appears when the particles move parallel with respect to each other. To deal with this divergences, one usually applies cuts, which filter events in the divergent region achieving convergence (See Table 2). This way a well-defined cross-section is calculated, but can be compared to experimental results only if the same cuts are applied to the data. In our case, the cuts applied to all particles in the final state are $E_i > 10\ GeV$ and $R_{ij} > 0.4$. Here, R_{ij} is defined as:

$$R_{ij} \equiv \sqrt{(\eta_i - \eta_j)^2 + (\phi_i - \phi_j)^2}, \tag{3}$$

where ϕ_i the azimuthal angle and η_i is the pseudorapidity of the ith particle:

$$\eta_i \equiv -\ln\left[\tan\left(\frac{\theta}{2}\right)\right], \tag{4}$$

with θ being the angle between the particle and the positive direction of the beam axis.

	`WHIZARD`	MadGraph
σ_{LO} (pb)	70.304 ± 0.083	70.24 ± 0.24

Table 1: Cross-section of the process $e^+\ e^- \to u\ \bar{u}\ g$ at $\sqrt{s} = 100\ GeV$.

2.2 Calculation of the NLO cross-section with Example

In the previous section we performed the calculation of the cross-section at LO (Born level) of the process $e^+\ e^- \to u\ \bar{u}\ g$. Now, we will try to understand how the NLO calculation works, which includes loop(virtual) diagrams and real tree-level diagrams of higher order. We will show one example of each diagram for the aforementioned process (Figures 3 and 4).

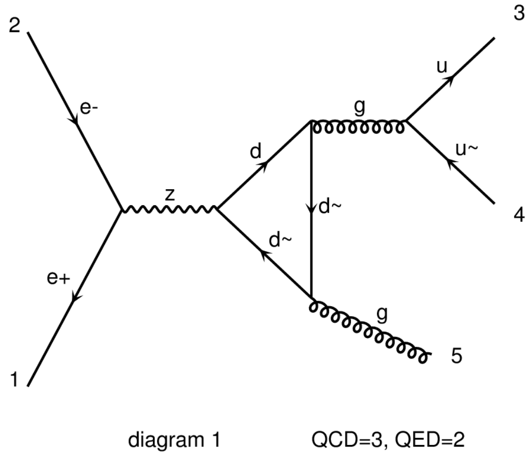

Figure 3: Example of Loop diagram

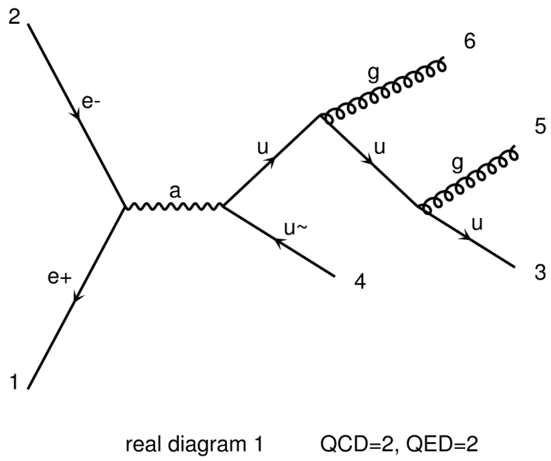

Figure 4: Example of Real diagram

Naively, the cross-section would have the following structure including the Born ($\mathcal{B}$) , Virtual ($\mathcal{V}$) and Real ($\mathcal{R}$) contributions:

$$d\sigma^{NLO} = d\sigma^{\mathcal{B}} + d\sigma^{\mathcal{R}} + d\sigma^{\mathcal{V}}. \tag{5}$$

However, the integration process is a little more complicated because the virtual and real terms are divergent by themselves.However, the KLN theorem [9] guarantees that the three contributions must be finite once suitable cuts are applied, which is assured by the finiteness of the LO cross section. The singularities in these cases are also infrared singularities, exactly as the ones of the previous section (collinear or soft). The problem can be solved solved by including a "Substraction term" ($\mathcal{S}$), that cancels the divergences:

$$d\sigma^{NLO} = d\sigma^{\mathcal{B}} + \left(d\sigma^{\mathcal{R}} - d\sigma^{\mathcal{S}}\right) + \left(d\sigma^{\mathcal{V}} + d\sigma^{\mathcal{S}}\right). \tag{6}$$

This Substraction term is calculated in `WHIZARD` using the FKS Scheme, explained in [10]. A substraction scheme basically consists on determining the values of $\mathcal{R}$ and $\mathcal{V}$ in the divergent limits and use them for the substraction. Table 2 shows the value of the cross-section of the previous process:

	LO	Real (substracted)	Virtual (substracted)	NLO
σ (pb)	3.7579 ± 0.0069	-0.2178 ± 0.0043	0.1872 ± 0.0014	3.7272 ± 0.0083

Table 2: LO, Real with substraction, Virtual with substraction and NLO Cross-sections of the process $e^+ \ e^- \to u \ \bar{u} \ g$ at $\sqrt{s} = 200 \ GeV$. The last column is the sum of the previous three in accordance with Equation 6.

2.3 $e^+ \ e^- \to b \ \bar{b} \ W^+ \ W^-$ at NLO QCD

Since some discrepancy has been found while studying the cross-section of this process when comparing to [1], it is interesting to compare `WHIZARD` 's result with MadGraph and see if they both agree. The parameters are taken from [1] and summarized here:

$$\begin{aligned} \alpha(m_Z)^{-1} = 127.918, \quad \alpha_s(m_Z^2) = 0.1176, \quad \Gamma_Z = 2.495 \ GeV, \\ \Gamma_W = 2.141 \ GeV, \quad m_t = 172.5 \ GeV, \ \Gamma_t = 1.3745 \ GeV^1, \\ m_H = 120 \ GeV, \quad \Gamma_H = 0.3692 \cdot 10^{-2} \ GeV \end{aligned}$$

The results for the cross-section at LO are:

$\sqrt{s}$ (GeV)	$\sigma_{LO}(fb)$		
	`WHIZARD`	MadGraph	Guo et al. [1]
1000	241.16 ± 0.52	240.5 ± 0.5	182.24 ± 0.07
1500	125.08 ± 0.26	124.4 ± 0.3	82.73 ± 0.03

Table 3: Comparison of the LO cross-section of the process $e^+ \ e^- \to b \ \bar{b} \ W^+ \ W^-$.

It is clear that both `WHIZARD` and Madgraph are consistent with each other. A possible explanation for the disagreement with [1] could be that they did not take into account diagrams including Higgs bosons. Such a result could be reproduced by letting the Higgs mass go to infinity, nevertheless we do not see a big change for $\sqrt{s} = 1000 \ GeV$ and

[1]It is the NLO width, calculated using the same formula as in [1].

$M_H = 1.2 \cdot 10^{12}\ GeV$:

$$\sigma_{Wh,M_H \to \inf} = 235.40 \pm 0.49\ fb, \tag{7}$$
$$\sigma_{MG,M_H \to \inf} = 235.3 \pm 0.6\ fb. \tag{8}$$

Let's now have a look to the cross-section at NLO. At $\sqrt{s} = 500\ GeV$, the results are:

	WHIZARD	MadGraph	Guo et al. [1]
$\sigma_{LO}\ (fb)$	673.27 ± 0.68	673.5 ± 1.3	602.57 ± 0.30
$\sigma_{NLO}\ (fb)$	551.7 ± 6.50	548 ± 20	575.5 ± 2.2

Table 4: Comparison of the NLO cross-section of the process $e^+\ e^- \to b\ \bar{b}\ W^+\ W^-$ at $\sqrt{s} = 500\ GeV$.

Moreover, a scan for increasing center-of-mass energies is displayed in Figure 5.

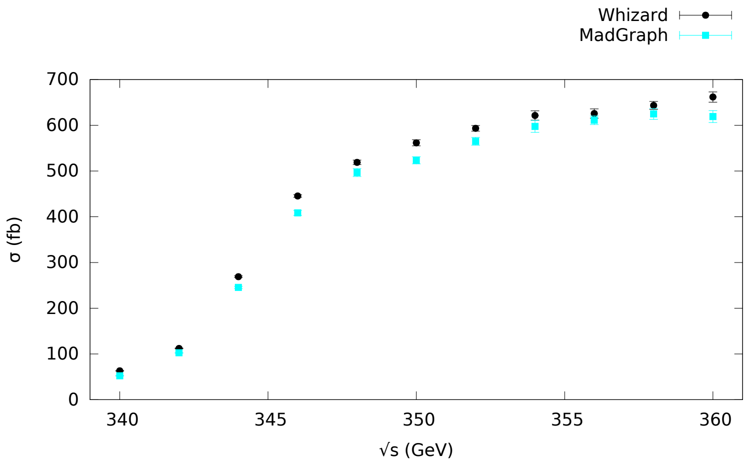

Figure 5: Cross-section at NLO for $e^+\ e^- \to b\ \bar{b}\ W^+\ W^-$ with scale $\mu = \sqrt{s}$.

As a conclusion for this process, we could affirm that there might be a problem in the calculations of [1], given the agreement at LO and NLO of two independent programs.

2.4 $e^+\ e^- \to jjjj$ and $e^+\ e^- \to jjj$

Let us now consider the case of electron-positron annihilation into four jets. What one sees experimentally is a cone of hadrons coming from a point due to the hadronization process of colour charged particles (q and g), so the theoretical calculation for this cross-section is obtained by considering $j = u, d, c, s, b, \bar{u}, \bar{d}, \bar{c}, \bar{s}, \bar{b}, g$. We use the FastJet [7] package, which is linked to WHIZARD , but only after performing some modifications in the code, so that the Aachen-Cambridge jet algorithm [11] can be used for electron positron collisions.

A jet algorithm is a procedure to find and separate jets in experimentation and in theory. Basically one imposes certain conditions to identify a jet as separate from others. In particular, the Cambridge-Aachen algorithm imposes for two jets namely i and j to be considered different that:

$$y_{ij} = \frac{2\min(E_i^2, E_j^2)}{Q^2}(1-\cos\theta_{ij}) > y_{cut}, \tag{9}$$

where Q is a reference scale, usually chosen to equal the renormalization scale. The algorithm matches the two jets into one if they don't fulfill the condition. This procedure is also strong enough to avoid collinear and soft divergences, because of the condition in θ and energy.
We compare the results obtained by using `WHIZARD` with [2] and [4]. Following their convention, we normalize our results to σ_{jj} (the LO cross-section of the process $e^+ e^- \to jj$), because this way the dependence on the electroweak coupling constants cancels. Our results at LO can be seen in Figure 6, and they are clearly compatible to the ones of [2] and [4]. Moreover, an equivalent result at LO can be obtained without any jet algorithm but just imposing a cut in which we impose the condition of Equation 9. At NLO, however, this would not lead to the same result, since in this situation there could be more than 5 jets in final state which can be matched together. For example, if two of the five jets were too close, it wouldn't pass the cut. However, the jet algorithm would match them together, having four jets in the final state, and so passing the cut.

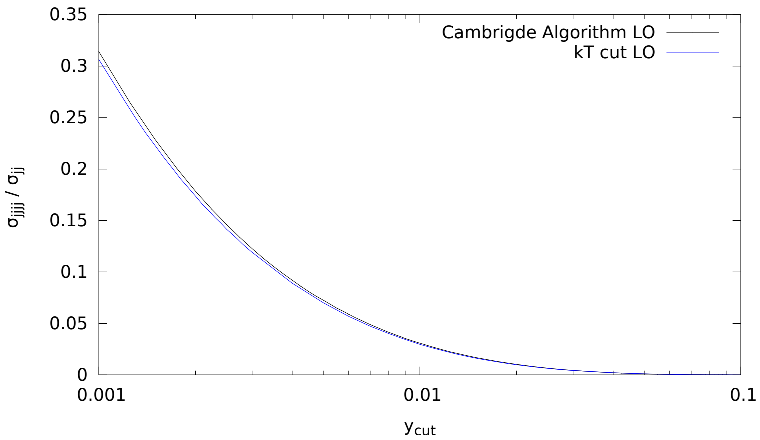

Figure 6: Cross-section at LO for $e^+ e^- \to jjjj$ with $\mu = \sqrt{s} = 91.187\ GeV = m_Z$ using Cambridge Algorithm for jet identification and a simple cut.

Besides, we studied what happens in the production of 3 jets. This result is again comparable to the one in [2].

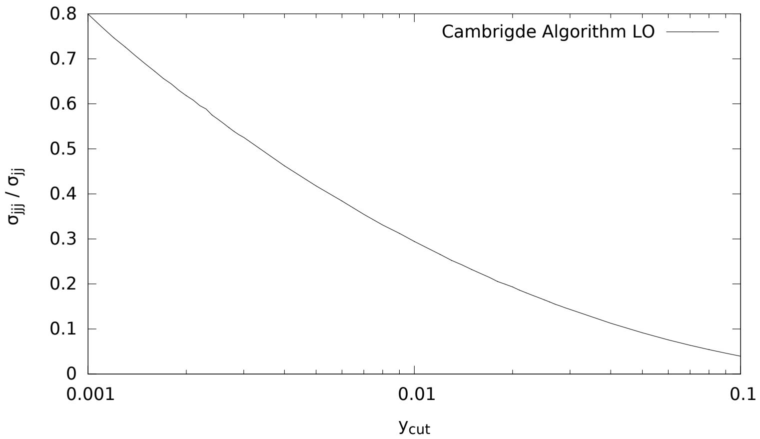

Figure 7: Cross-section at LO for $e^+ \, e^- \rightarrow jjj$ with $\mu = \sqrt{s} = 91.187 \; GeV = m_Z$ using Cambridge Algorithm for jet identification.

3 Conclusion

WHIZARD is a powerful tool for cross section calculation and event simulation. Nevertheless, NLO calculations are an experimental feature which naturally contains bugs and hidden problems and therefore, validation and feedback is essential to improve it.
During the validation a few bugs were found and communicated, so that they could be solved. The majority of the errors were found during calculations at NLO. However, some of them could not be solved as quickly, for instance, the calculation at NLO of four jets production. In this particular case, two issues arose. First, the clustering FastJet algorithm at NLO does not seem to work as at LO and does not achieve convergence. Second, the flavour structure of the 4 jets at NLO includes some processes having order 4 in the EW coupling, whereas it should only include order 2 in both strong and WE couplings.
Of course, the validation task is far from being complete. More processes have to be calculated, focusing on NLO, so that further problems come out. Moreover, for experimental features, feedback from the users is required.

4 Acknowledgement

Special thanks to Christian Weiss, who helped me a lot and was always available.
I would also like to show my gratitude to Jürgen Reuter for the time invested in the supervision of my project.
To conclude, I would like to thank my office mates Thanat and Augustinas, because work with you was less tough.

References

[1] L. Guo, W. G. Ma, R. Y. Zhang and S. M. Wang, Phys. Lett. B **662** (2008) 150 [arXiv:0802.4124 [hep-ph]].

[2] Z. Nagy and Z. Trocsanyi, Nucl. Phys. Proc. Suppl. **74** (1999) 44 [hep-ph/9808364].

[3] F. Cascioli, P. Maierhofer and S. Pozzorini, Phys. Rev. Lett. **108** (2012) 111601 [arXiv:1111.5206 [hep-ph]].

[4] Z. Nagy and Z. Trocsanyi, Phys. Rev. D **59** (1999) 014020 [Phys. Rev. D **62** (2000) 099902] [hep-ph/9806317].

[5] W. Kilian, T. Ohl and J. Reuter, Eur. Phys. J. C **71** (2011) 1742 [arXiv:0708.4233 [hep-ph]].

[6] M. Moretti, T. Ohl and J. Reuter, In *2nd ECFA/DESY Study 1998-2001* 1981-2009 [hep-ph/0102195].

[7] M. Cacciari, G. P. Salam and G. Soyez, Eur. Phys. J. C **72** (2012) 1896 [arXiv:1111.6097 [hep-ph]].

[8] J. Alwall *et al.*, JHEP **1407** (2014) 079 [arXiv:1405.0301 [hep-ph]].

[9] T. Kinoshita, J. Math. Phys. **3** (1962) 650.

[10] S. Frixione, P. Nason and C. Oleari, JHEP **0711** (2007) 070 [arXiv:0709.2092 [hep-ph]].

[11] Y. L. Dokshitzer, G. D. Leder, S. Moretti and B. R. Webber, JHEP **9708** (1997) 001 [hep-ph/9707323].